

Numerical Exposure Investigation of a WPT Charger

Report

Order No. #6220425, Molex Technologies GmbH

Document Version 1.0 / 11th Apr, 2023

Authors: David Schäfer, Winfried Simon



IMST GmbH
Carl-Friedrich-Gauß-Str. 2-4
47475 Kamp-Lintfort
Germany



Information

File Name	Report_WCH-304_V1.0.pdf
Initial Date	11th Apr, 2023
Page count	26

Versions

Release Date	Version	Author	Comments
11th Apr, 2023	1.0	David Schäfer	Initial version

Approval

Name	Job Title	Date	Signature
David Schäfer	Project leader, study director	11th Apr, 2023	
Winfried Simon	Approval	11th Apr, 2023	

Device Under Test (DUT)

Type of DUT	Wireless Power Transfer Charger
Model Name	WCH-304
FCC ID	RK7WCH-304
ISED Certification No.	4774A-WCH304
Frequency Band	127.55 kHz
Antennas / Coils / Active Elements	Three coils
Applicant	Molex Technologies GmbH Mizarstrasse 3 12529 Schönefeld, Germany Contact: Ines Baufeld

Evaluation Results

Quantity inside flat phantom	Result*	Below exposure limit set by ...				
		ICNIRP 2020	47 CFR § 1.1310	RSS-102 Issue 5	1999/519/EC	RPS S-1
SAR _{1g, max}	84.2357 mW/kg	—**	Yes	Yes	—	—
SAR _{10g, max}	40.5715 mW/kg	Yes	Yes	Yes	Yes	Yes
EIAV _{max}	15.8004 V/m	—	—	Yes	—	Yes

* Simulated values for "reported model", cf. section 3.2
 ** Not applicable combinations were indicated as "—"

Human Exposure Limits

Specific Absorption Rate (ICNIRP 2020, 1999/519/EC, RPS S-1)

Condition	Uncontrolled Environment (General Public)		Controlled Environment (Occupational)	
	SAR Limit	Mass Avg.	SAR Limit	Mass Avg.
SAR averaged over the whole body mass	0.08 W/kg	whole body	0.4 W/kg	whole body
Peak spatially-averaged SAR for the head, neck & trunk	2.0 W/kg	10 g of tissue*	10 W/kg	10 g of tissue*
Peak spatially-averaged SAR in the limbs/extremities	4.0 W/kg	10 g of tissue*	20 W/kg	10 g of tissue*

* Defined as a tissue volume in the shape of a cube

Specific Absorption Rate (RSS-102 Issue 5)

Condition	Uncontrolled Environment (General Public)		Controlled Environment (Occupational)	
	SAR Limit	Mass Avg.	SAR Limit	Mass Avg.
SAR averaged over the whole body mass	0.08 W/kg	whole body	0.4 W/kg	whole body
Peak spatially-averaged SAR for the head, neck & trunk	1.6 W/kg	1 g of tissue*	8 W/kg	1 g of tissue*
Peak spatially-averaged SAR in the limbs/extremities	4.0 W/kg	10 g of tissue*	20 W/kg	10 g of tissue*

* Defined as a tissue volume in the shape of a cube

Specific Absorption Rate (47 CFR Ch. I § 1.1310 10-1-20 Edition)

Condition	Uncontrolled Environment (General Public)		Controlled Environment (Occupational)	
	SAR Limit	Mass Avg.	SAR Limit	Mass Avg.
SAR averaged over the whole body mass	0.08 W/kg	whole body	0.4 W/kg	whole body
Peak spatially-averaged SAR	1.6 W/kg	1 g of tissue*	8 W/kg	1 g of tissue*
Peak spatially-averaged SAR for extremities, such as hands, wrists, feet, ankles, and pinnae	4.0 W/kg	10 g of tissue*	20 W/kg	10 g of tissue*
* Defined as a tissue volume in the shape of a cube				

Internal Electric Field (ICNIRP 2020)

Condition	Uncontrolled Environment (General Public)	Controlled Environment (Occupational)
	EIAV Limit	EIAV Limit
Peak EIAV @ 100 kHz - 10 MHz	$1.35 \cdot 10^{-4} \cdot f \text{ V/m}^*$	$2.7 \cdot 10^{-4} \cdot f \text{ V/m}^*$
Peak EIAV @ 127.55 kHz	17.21925 V/m	34.4385 V/m
* Frequency f in Hz		
** Not applicable combinations were indicated as "—"		

Internal Electric Field (RSS-102 Issue 5, RPS S-1)

Condition	Uncontrolled Environment (General Public)	Controlled Environment (Occupational)
	EIAV Limit	EIAV Limit
Peak EIAV @ 3 kHz - 10 MHz	$1.35 \cdot 10^{-4} \cdot f \text{ V/m}^*$	$2.7 \cdot 10^{-4} \cdot f \text{ V/m}^*$
Peak EIAV @ 127.55 kHz	17.21925 V/m	34.4385 V/m
* Frequency f in Hz		

Contents

1	Introduction	6
1.1	Objective	6
1.2	Simulation Method	6
1.3	DUT Description	6
1.4	Setup for Reference Measurement	6
2	EM Simulation Model	8
2.1	Model Setup	8
2.2	Model Check	9
2.2.1	Magnetic Fields	9
2.2.2	Coil Inductance	12
2.2.3	Conclusion of Model Validation	12
3	SAR and EIAV Evaluation	13
3.1	Simulation Results	14
3.2	Simulation Uncertainty	15
3.2.1	Simulation Parameter Related Uncertainty	15
3.2.2	Model Related Uncertainty	18
3.2.3	Model Validation	19
3.2.4	Uncertainty Budget	20
3.2.5	Uncertainty Penalty	20
3.3	Passive Receiver Impact	20
3.4	Conclusion of SAR and EIAV Evaluation	23
4	Appendix	24
4.1	Specific Information for Computational Modelling	24
4.2	Abbreviations	25
5	References	26

List of Figures

1	Photo of the DUT	7
2	Measurement setup CTC	7
3	Geometry of the model - outer	8
4	Geometry of the model - internal	9
5	Geometry of the model - exploded	10

6	Magnetic field plane	11
7	Line evaluation, graph	11
8	Geometry of the phantom	13
9	Simulated 1g-averaged SAR results	14
10	Simulated EIAV results	15
11	Geometry of the passive receiver dummy	22
12	EIAV for the model with the passive receiver dummy	22

List of Tables

1	Coil inductance from datasheet, measurement and simulation.	12
2	SAR and EIAV maximum values	14
3	Uncertainty Budget Procedure	16
4	SAR and EIAV results for different phantom positions	16
5	SAR and EIAV results for different mesh resolutions	16
6	EIAV results for different simulation domain sizes	17
7	SAR and EIAV results for different number of total time steps	17
8	Uncertainty budget, simulation parameters, 1g-SAR	17
9	Uncertainty budget, simulation parameters, 10g-SAR	18
10	Uncertainty budget, simulation parameters, EIAV	18
11	Uncertainty budget, model setup	19
15	Influence of passive receiver dummy on SAR and EIAV	20
12	Combined and expanded uncertainty, 1g-SAR	21
13	Combined and expanded uncertainty, 10g-SAR	21
14	Combined and expanded uncertainty, EIAV	21
16	Abbreviations	25

1 Introduction

1.1 Objective

The objective of this report is the numerical exposure investigation of one Wireless Power Transfer (WPT) charger (further referred to as "device under test" or "DUT") designed by Molex Technologies GmbH (further referred to as "applicant"). In particular the Specific Absorption Rate (SAR, heat damage hazard) and internal electric fields (EIAV¹, instantaneous nerve stimulation hazard) was investigated and compared to exposure limits specified by ICNIRP [1], FCC [2], ISED [3], EUCO [5] and the ARPANSA [6].

1.2 Simulation Method

All simulations were done with the Finite Difference Time Domain (FDTD) simulation tool Empire XPU [7]. A numerical model of the DUT was generated and validated by measurements of the magnetic field in its vicinity and measured inductance of the charging coil. The SAR and EIAV inside a flat phantom (human body part model) were investigated similar to the assessment procedures described in IEC/IEEE 62704-1 [8, 9]. The procedures were adapted to make them suitable for the low frequency of the DUT.

1.3 DUT Description

The 15 W, triple coil, WPT charger "WCH-304" (further referred to as "device under test" or "DUT") can be used to charge portable devices like smart-phones (further referred to as "WPT receiver"). It is designed to be integrated into a vehicle, e.g. into the center console of a car. The DUT operates at a frequency of 127.55 kHz and features three charging coils. During operation only one of the three coils is excited/charging at a time. Which coil is used for charging is chosen by the DUT itself, depending on the placement of the WPT receiver device. A photo of the DUT is depicted in Figure 1.

1.4 Setup for Reference Measurement

A validation of the numerical model was carried out by comparing the simulated magnetic field in the vicinity of the DUT with a reference measurement. The measurement was done on the behalf of the applicant by the lab of "cetecom advanced GmbH"² with the setup depicted in Figure 2. They used a "DASY8" positioner system from Speag and a "MAGPy-H3D" magnetic field probe with a 1 cm² sensor size (loop) and 6.6 mm sensor center to tip distance. The measurements were done for a series production equivalent device, running in a testing operating mode at a fixed coil current of 4.5715 A(RMS). The applicant pre-determined this to be the maximum expectable coil current during charging a WPT receiver. After the measurements were already performed

¹EIAV is the particular name of the post-processing/visualisation feature in Empire XPU. The averaging is optional and was disabled for this investigation.

²The company "cetecom advanced GmbH" was known as "CTC advanced GmbH" and "CETECOM GmbH" before their fusion in January 2023.



Figure 1: Photo of the DUT

the value was corrected to 4.3 A (RMS) by the applicant and the measurement results were scaled down accordingly with a factor of $4.3/4.5715 = 0.9406$. No WPT receiver was present during the reference measurements of the magnetic field.

At first "cetecom advanced GmbH" determined by H-field measurements that the strongest fields occur when coil 3 (towards the external connector) is excited, so this operation state was considered throughout the investigation. For the reference measurement the field probe was located directly above the xy -center of the active coil. A line measurement of the magnetic field strength was performed by lifting the probe upwards to different z -distances from the DUT. Figure 2 (a) shows the lowest possible position of the field probe (touch position).



(a)



(b)

Figure 2: Measurement setup from the external lab of "cetecom advanced GmbH", showing (a) a close-up of the "MAGPy-H3D" probe in touch position and (b) the "DASY8" positioner.

2 EM Simulation Model

2.1 Model Setup

The simulation model of the DUT is based on STEP CAD data, PCB layout data, technical drawings and photos provided by the applicant. First the CAD- and layout data was imported into Empire XPU and then rotated/moved, so that the center of the DUTs top surface became the coordinate origin of the numerical model. Figure 3 shows a top and bottom 3D view of the simulation model.

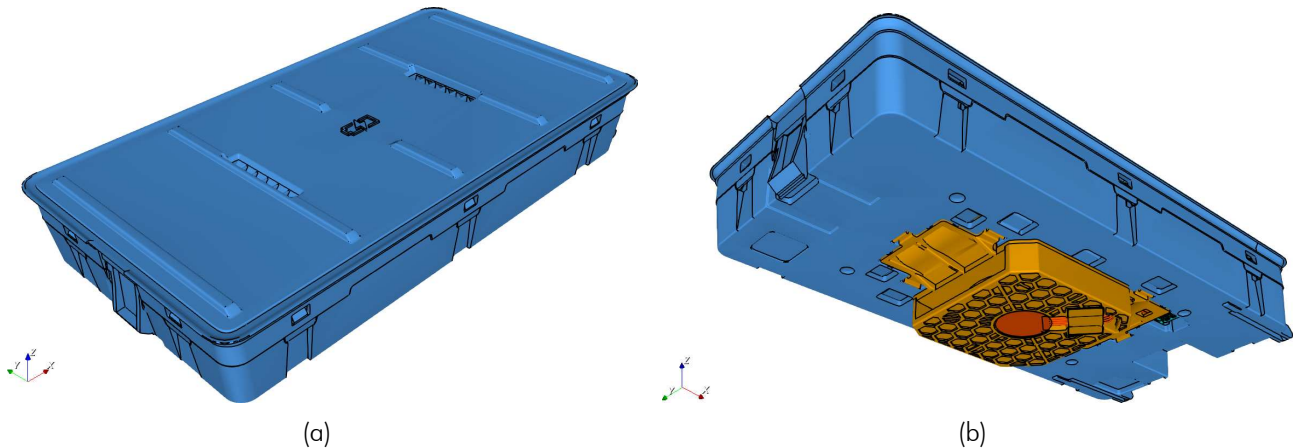


Figure 3: Geometry of the Empire simulation model of the DUT, showing the outer view on the top (a) and bottom (b) side.

In Figure 4 the internal components are visible, including the three WPT charging coils (in colors red / yellow / blue). The charging coil (coil 3) can be seen on the left (red), overlapping the center coil. The middle point of the active coil is located at $x = -14.01$ mm, $y = 0$ mm, $z = -6.58$ mm and the top side of the DUT housing is at $z = 0.0$ mm.

Figure 5 shows an exploded view of the most important components of the simulation model. Based on the applicants information the material properties were set as follows:

- (a) Top housing (PC+ABS, $\epsilon_r = 3.1$, $\tan(\delta) = 0.01$)
- (b) Top PCB (Copper traces, $\sigma = 59.6 \cdot 10^6$ S/m)
- (c) Top PCB components (PEC, $\sigma = Inf$)
- (d) Coilframe (PC+ABS, $\epsilon_r = 3.1$, $\tan(\delta) = 0.01$)
- (e) WPT coils ($\sigma = 14.2 \cdot 10^6$ S/m)
- (f) Ferrite plate ($\mu_r = 2700$, $\tan(\delta) = 0.0162$)
- (g) Bottom PCB (Copper traces, $\sigma = 59.6 \cdot 10^6$ S/m)
- (h) Bottom PCB components (PEC, $\sigma = Inf$)
- (i) Bottom PCB shielding (1.0372 steel, $\sigma = 1.45 \cdot 10^6$ S/m)
- (j) Bottom housing (PC+ABS, $\epsilon_r = 3.1$, $\tan(\delta) = 0.01$)
- (k) Cooling fan (PC+ABS, $\epsilon_r = 3.1$, $\tan(\delta) = 0.01$ and PEC, $\sigma = Inf$)

From the top PCB the vias (through connections) between top and bottom layer were removed from the simulation model, because they have a negligible effect on the assessed quantities but require an excessively fine mesh for preventing false short circuits.

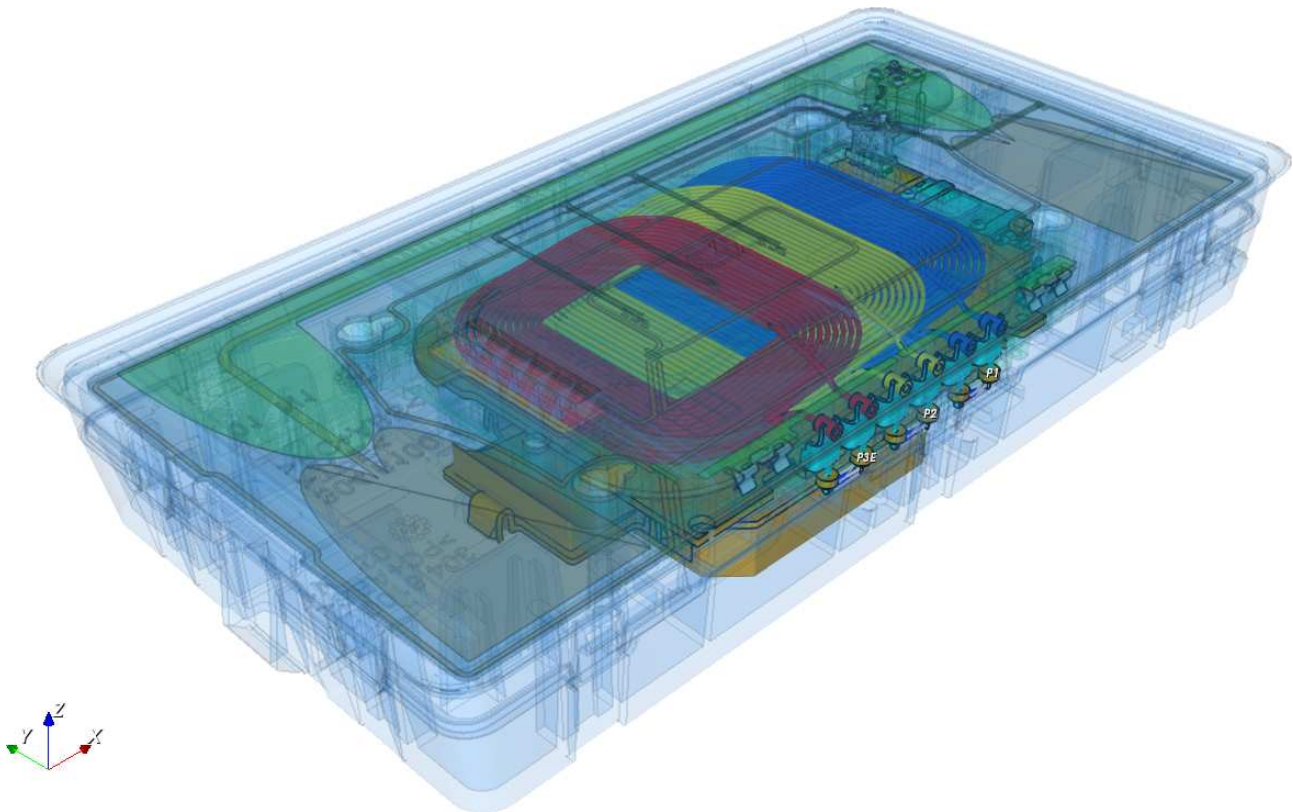


Figure 4: Geometry of the Empire simulation model of the DUT. The housing of the DUT is set transparent to show the internal components.

2.2 Model Check

The simulation model was checked by comparing the simulated magnetic fields with the reference measurement (cf. section 1.4). During measurement the active coil was excited with the maximum expectable current of 4.3 A (RMS) at a frequency of 127.55 kHz. The two other coils were inactive, so during the simulation their inputs were terminated with non-excited ports with 100 k Ω impedance. The simulation setup was unperturbed, meaning that it didn't include a WPT receiver device or phantom (human body model).

2.2.1 Magnetic Fields

Figure 6 shows a yz -cutplane for the simulated magnetic field strength through the center of the DUT. It can be seen how the main PCBs ground and the ferrite confine the main part of the magnetic field to the dedicated WPT receiver location above the DUT.

Analogue to the setup of the measurement (cf. section 1.4) the simulated magnetic field (H-field) strength was evaluated along the corresponding line above the active coil. The measurements start at $z = 6.6$ mm, which corresponds to the "sensor center to tip distance" of the "MAGPy-H3D" field probe. The simulated line starts at the top of the DUTs housing at ($z = 0$ mm). As Figure 7 depicts, the simulated H-field is in very good agreement with the measurement.

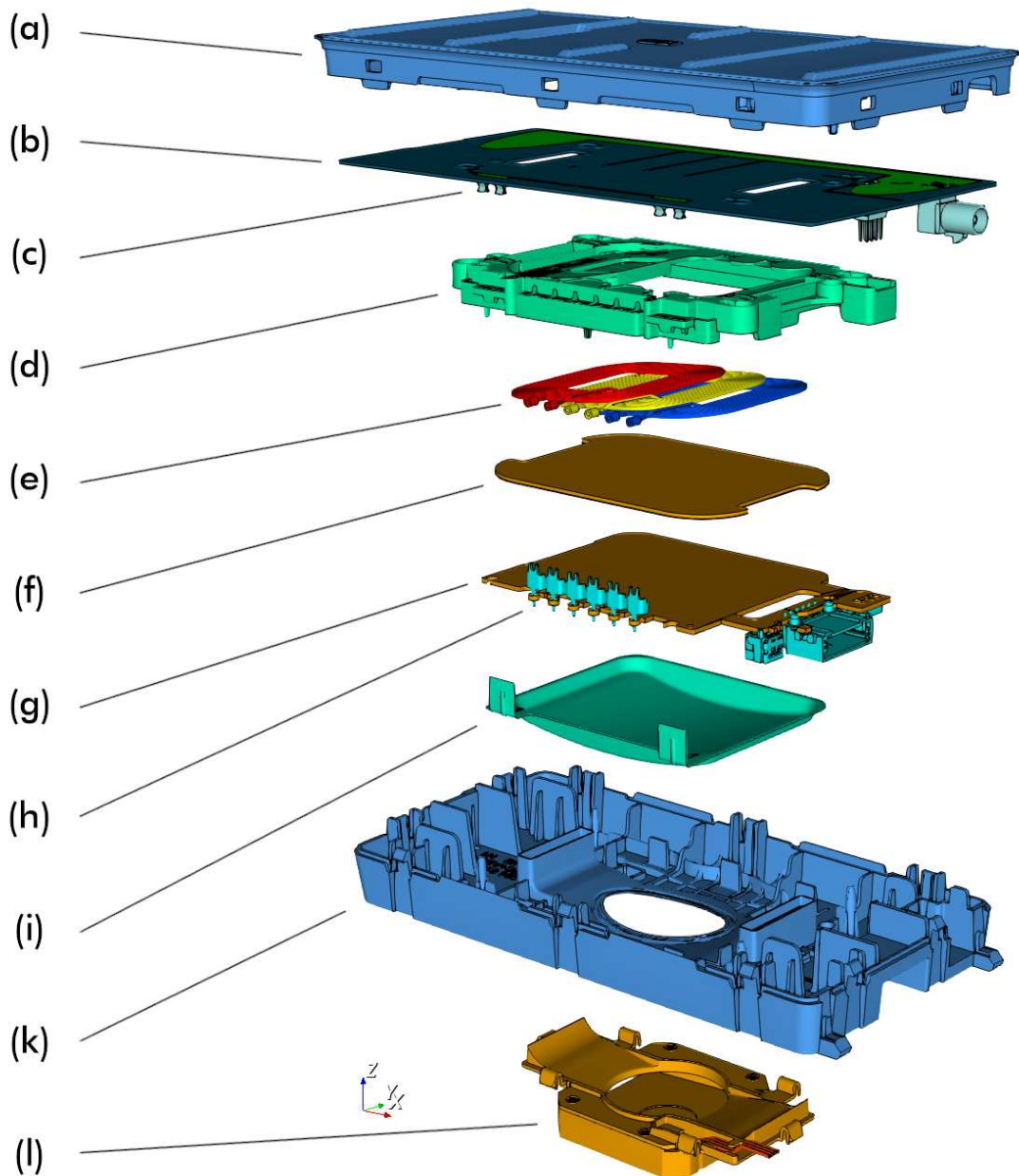


Figure 5: Geometry of the Empire simulation model of the DUT, showing an exploded view of the top housing (a), the top PCB (b), the top PCB components (c), the coilframe (d), the WPT coils (e), the ferrite (f), the bottom PCB (g), the bottom PCB components (h), the bottom PCB shielding (i), the bottom housing (k) and the cooling fan (l).

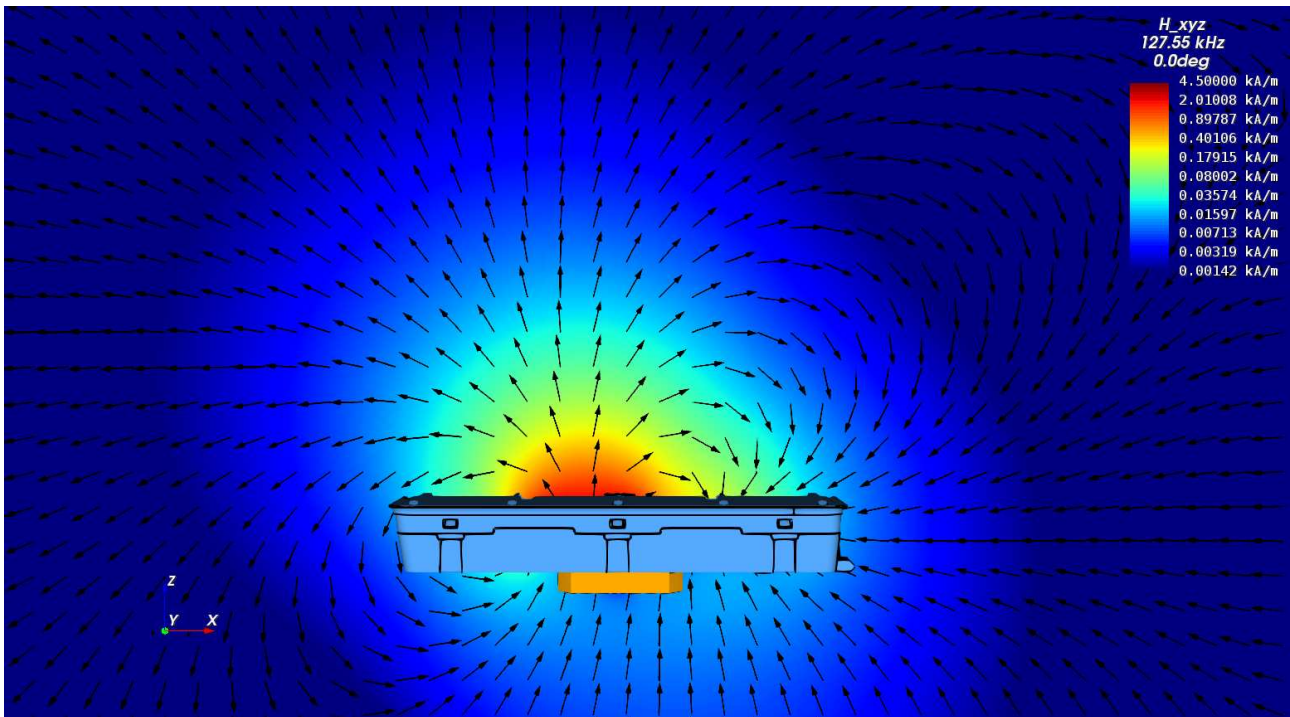


Figure 6: The simulated magnetic field displayed on a yz -plane through the DUT.

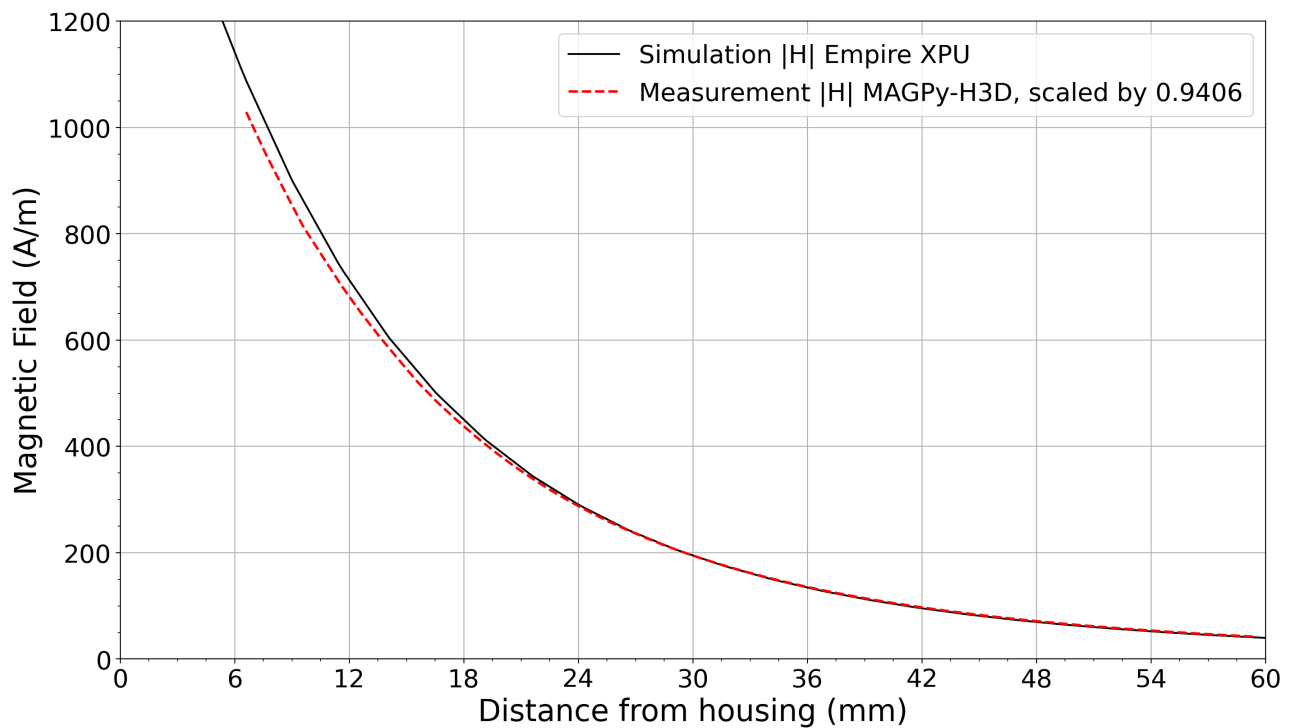


Figure 7: Curves for the line evaluation of the H-field (RMS values). The top of the DUT dielectric housing is located at $z = 0.0$ mm. The measurement results were scaled by a factor of 0.9406 for the reason explained in section 1.4

2.2.2 Coil Inductance

In addition to the magnetic fields also the inductance of the coil was used to check the simulation model. Due to the applicant the coil modules (coils and ferrite) datasheet states an expectable inductance of $11.5\mu\text{H} \pm 10\%$, and they measured an average value of $10.930\mu\text{H}$ for an assembled coil module with shielding cap. The simulated inductance of $11.468\mu\text{H}$ is in good agreement with this values, showing a relative deviation of 4.922% from the measured value.

	Datasheet	Measurement	Empire
Coil Inductance	$11.5\mu\text{H} \pm 10\%$ = $[10.35\mu\text{H}; 12.65\mu\text{H}]$	$10.930\mu\text{H}$	$11.468\mu\text{H}$

Table 1: Coil inductance from datasheet, measurement and simulation.

2.2.3 Conclusion of Model Validation

It can be concluded, that simulated magnetic field strength and inductance are in good agreement (cf. Figure 7 and Table 1) with the measurements from the applicant and the external lab of "cetecom advanced GmbH", indicating the accurate setup of the Empire simulation model.

3 SAR and EIAV Evaluation

For the evaluation of the Specific Absorption Rate (SAR) and the internal Electric field (EIAV) a box shaped flat phantom was added to the simulation model. The setup resembles the situation of someone touching the DUT just after a receiver removal which was in "charging mode" at maximum field. The continuous maximum expectable coil current of 4.3 A (RMS) was retained throughout the investigation.

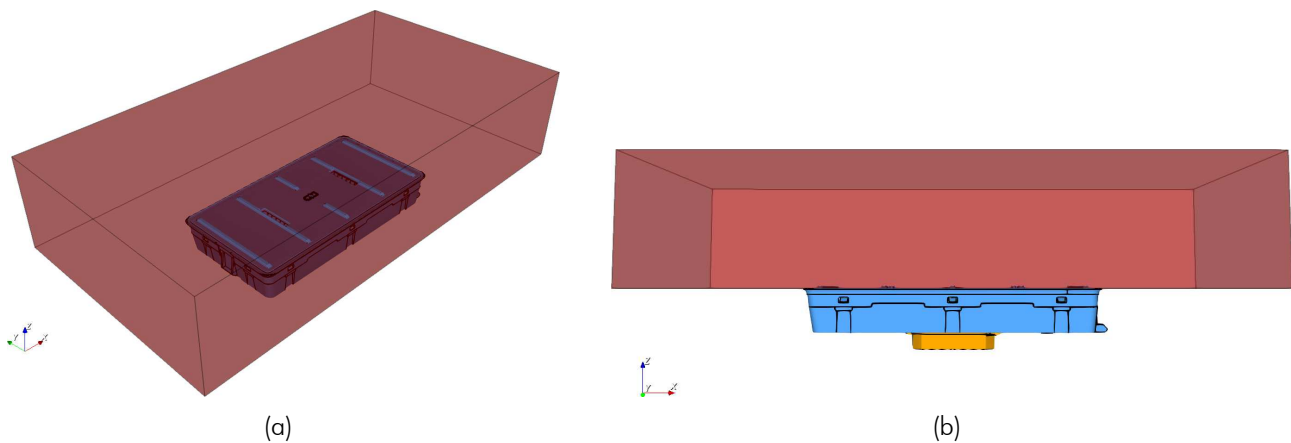


Figure 8: Geometry of the flat phantom in 3D view (a) and side view (b) showing it is in touch with the DUTs housing.

The phantom was centered (xy -direction) above the DUT at closest possible z -distance, virtually touching the basis of the top side of the DUTs dielectric housing as shown in Figure 8. In the sense of the worst-case consideration small protruding features³ were overwritten by the phantom to realize closest possible phantom positioning. With respect to the CAD coordinate system origin, the phantom's bottom side (side towards DUT) is located at $z = 0$ mm. The dimensions and the material properties of the phantom are as follows:

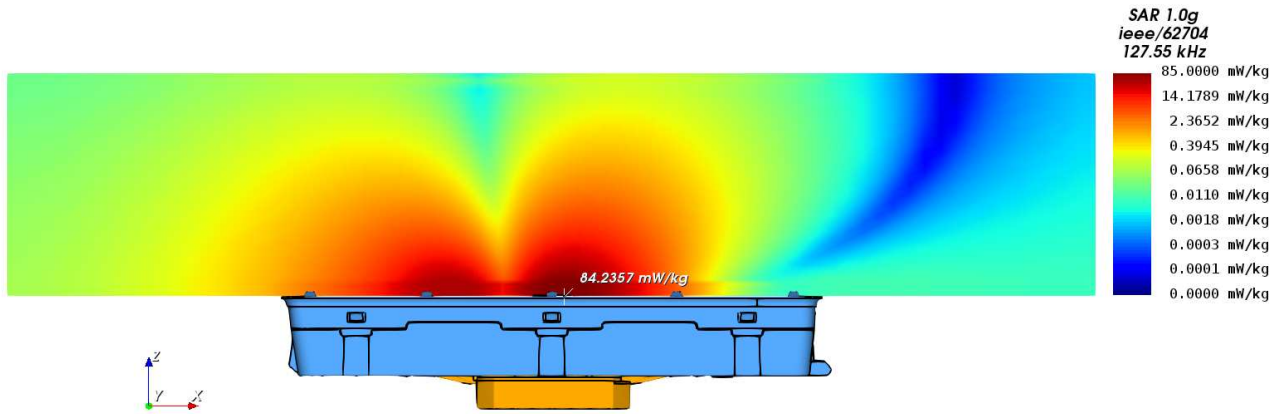
1. Geometric Size: $d_x \cdot d_y \cdot d_z = 350 \text{ mm} \cdot 180 \text{ mm} \cdot 72 \text{ mm}$
2. Relative Permittivity: $\epsilon_r = 55$
3. Electrical Conductivity: $\sigma = 0.75 \text{ S/m}$
4. Mass Density: $\rho = 1000 \text{ kg/m}^3 = 1 \text{ g/cm}^3$

More details about the numerical model, like e.g. domain size, time step or total number of mesh cells, can be found in the appendix in section 4.1.

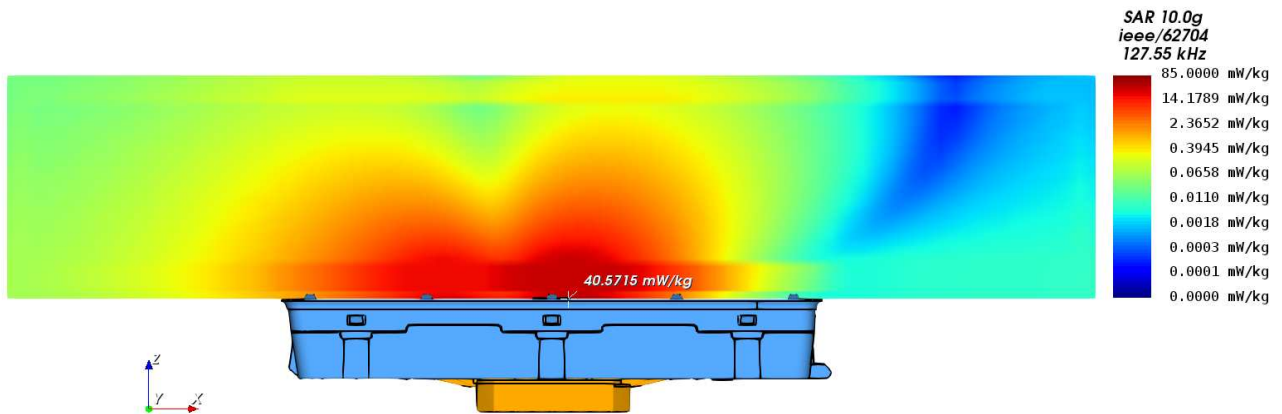
³For example the two rims that ensure a small air gap between the DUT and a WPT receiver for cooling purposes.

3.1 Simulation Results

Figure 9 shows the simulated 1g- and 10g-averaged SAR and Table 2 lists the corresponding maximum values and their positions. Figure 10 shows the simulated un-averaged EIAV and Table 2 lists the corresponding maximum value and its position.



(a) Simulated 1g-averaged SAR



(b) Simulated 10g-averaged SAR

Figure 9: Cutplanes through the maxima of the simulated 1g-averaged SAR (a) and 10g-averaged SAR (b) inside the flat phantom. The phantom geometry is not visible. The discontinuities at the phantom boundaries are caused by the averaging algorithm (cf. [8, Section 6.2.2]).

Quantity	Maximum Value	Position of Maximum		
		x	y	z
$SAR_{1g, \max}$	84.2357 mW/kg	4.32715 mm	-0.472538 mm	0.125 mm
$SAR_{10g, \max}$	40.5715 mW/kg	5.41260 mm	-0.472538 mm	0.125 mm
$EIAV_{\text{unaveraged}, \max}$	15.8004 V/m	3.96926 mm	-0.472538 mm	0.125 mm

Table 2: SAR and EIAV maximum values with their corresponding positions.

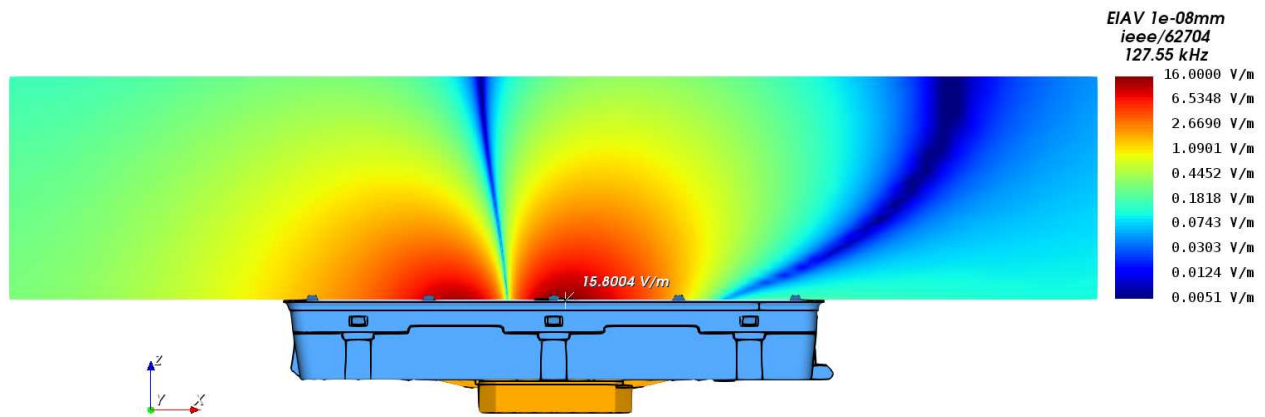


Figure 10: Cutplane through the maximum of the simulated EIAV inside the flat phantom. The phantom geometry is not visible.

3.2 Simulation Uncertainty

Based on chapter 7 of IEC/IEEE 62704-1 [8] the Combined- and Expanded Standard Uncertainty was calculated to analyse the accuracy of the results for the numerical model (further referred to as "reported model"). Because the DUTs operating frequency is below the scope of the standard, the procedure had to be modified. Details about this will be described in the following sections.

3.2.1 Simulation Parameter Related Uncertainty

The procedure for evaluating the simulation parameter related uncertainty (IEC/IEEE 62704-1 [8, section 7.2]) was modified as described in Table 3. The Tables 4, 5, 6 and 7 show the maximum SAR and EIAV for the investigated variants as well as their relative deviation from the reported model. Table 10 shows the budget of the SAR and EIAV uncertainty contributions of the simulation parameters.

Uncertainty Component	Applicability of the Procedure from IEC/IEEE 62704-1 [8, section 7.2]	Nr. of Variations
Positioning	Applicable. Variation will be: Increase of distance between phantom and DUT by +1 mesh step	1
Mesh Resolution	Not 1:1 applicable. Requested refinement is not practicable at 127.55 kHz. Instead, total number of mesh cells is increased by a factor of 2	1
Boundary Condition	Not 1:1 applicable, because $\lambda/4 @ 127.55 \text{ kHz} = 588 \text{ m}$ is way too large. Instead, simulation domain is enlarged by 50% simultaneously in +/- x/y/z direction	1
Power Budget	Not applicable. No travelling wave conditions are given, so comparison with power absorbed in ABC is not possible. Excitation will be normalized to fixed port/coil current.	0
Convergence	Not 1:1 applicable. Instead, variation is simulated longer by a factor of 1.5 or more.	1
Phantom dielectrics	Not applicable / not indicated because fixed permittivity and conductivity from IEC/TR 62905 were used.	0

Table 3: Description of the modified procedure for obtaining the uncertainty budget.

Phantom z-Position	0.00 mm	0.25 mm
$SAR_{1g, \max}$	84.2357 mW/kg	80.8357 mW/kg
$SAR_{10g, \max}$	40.5715 mW/kg	39.1118 mW/kg
$EIAV_{\max}$	15.8004 V/m	15.4399 V/m
$SAR_{1g, \max}$ -Deviation	0 %	-4.04 %
$SAR_{10g, \max}$ -Deviation	0 %	-3.60 %
EIAV-Deviation	0 %	-2.28 %

Table 4: SAR and EIAV results for different phantom positions. The first data column corresponds to the reported model (cf. section 3.1).

Mesh Resolution	12.7 MCells	27.1 MCells
$SAR_{1g, \max}$	84.2357 mW/kg	84.7577 mW/kg
$SAR_{10g, \max}$	40.5715 mW/kg	40.6353 mW/kg
$EIAV_{\max}$	15.8004 V/m	15.8137 V/m
$SAR_{1g, \max}$ -Deviation	0 %	0.62 %
$SAR_{10g, \max}$ -Deviation	0 %	0.16 %
EIAV-Deviation	0 %	0.08 %

Table 5: SAR and EIAV results for different mesh resolutions. The first data column corresponds to the reported model (cf. section 3.1).

Domain Size	550 · 380 · 389 mm	1100 · 760 · 778 mm
SAR _{1g, max}	84.2357 mW/kg	84.2898 mW/kg
SAR _{10g, max}	40.5715 mW/kg	40.5991 mW/kg
EIAV _{max}	15.8004 V/m	15.8055 V/m
SAR _{1g, max} -Deviation	0 %	0.06 %
SAR _{10g, max} -Deviation	0 %	0.07 %
EIAV-Deviation	0 %	0.03 %

Table 6: EIAV results for different simulation domain sizes. The first data column corresponds to the reported model (cf. section 3.1). The simulation domain was enlarged symmetrically in all spatial directions.

Time/Convergence	15 Msteps	25 Msteps
Energy Decay	−101.27 dB	−101.90 dB
SAR _{1g, max}	84.2357 mW/kg	84.2392 mW/kg
SAR _{10g, max}	40.5715 mW/kg	40.5720 mW/kg
EIAV _{max}	15.8004 V/m	15.7936 V/m
SAR _{1g, max} -Deviation	0 %	0.00 %
SAR _{10g, max} -Deviation	0 %	0.00 %
EIAV-Deviation	0 %	−0.04 %

Table 7: SAR and EIAV results for different number of total time steps. The first data column corresponds to the reported model (cf. section 3.1).

Uncertainty Component	Section in [8]	1g-SAR Tolerance in %	Probability Distribution	Divisor	c_i	1g-SAR Uncertainty in %
Positioning	7.2.1	−4.04 %	R	1.73	1	−2.33 %
Mesh Resolution	7.2.2	0.62 %	N	1	1	0.62 %
Boundary Condition	7.2.3	0.06 %	N	1	1	0.06 %
Power Budget	7.2.4	<i>not appl.</i>	N	1	1	<i>not appl.</i>
Convergence	7.2.5	0.00 %	R	1.73	1	0.00 %
Phantom dielectrics	7.2.6	<i>not appl.</i>	R	1.73	1	<i>not appl.</i>
Combined Std. Uncertainty (k=1)						2.41 %

Table 8: Budget of the 1g-SAR uncertainty contributions of the simulation parameters, corresponding to IEC/IEEE 62704-1 [8, Table 3]. Note: N, R, U = normal, rectangular, U-shaped probability distributions.

Uncertainty Component	Section in [8]	10g-SAR Tolerance in %	Probability Distribution	Divisor	c_i	10g-SAR Uncertainty in %
Positioning	7.2.1	-3.60 %	R	1.73	1	-2.08 %
Mesh Resolution	7.2.2	0.16 %	N	1	1	0.16 %
Boundary Condition	7.2.3	0.07 %	N	1	1	0.07 %
Power Budget	7.2.4	<i>not appl.</i>	N	1	1	<i>not appl.</i>
Convergence	7.2.5	0.00 %	R	1.73	1	0.00 %
Phantom dielectrics	7.2.6	<i>not appl.</i>	R	1.73	1	<i>not appl.</i>
Combined Std. Uncertainty (k=1)						2.09 %

Table 9: Budget of the 10g-SAR uncertainty contributions of the simulation parameters, corresponding to IEC/IEEE 62704-1 [8, Table 3]. Note: N, R, U = normal, rectangular, U-shaped probability distributions.

Uncertainty Component	Section in [8]	EIAV Tolerance in %	Probability Distribution	Divisor	c_i	EIAV Uncertainty in %
Positioning	7.2.1	-2.28 %	R	1.73	1	-1.32 %
Mesh Resolution	7.2.2	0.08 %	N	1	1	0.08 %
Boundary Condition	7.2.3	0.03 %	N	1	1	0.03 %
Power Budget	7.2.4	<i>not appl.</i>	N	1	1	<i>not appl.</i>
Convergence	7.2.5	-0.04 %	R	1.73	1	-0.02 %
Phantom dielectrics	7.2.6	<i>not appl.</i>	R	1.73	1	<i>not appl.</i>
Combined Std. Uncertainty (k=1)						1.32 %

Table 10: Budget of the EIAV uncertainty contributions of the simulation parameters, analogue to the budget of the SAR uncertainty contributions of the simulation parameters to IEC/IEEE 62704-1 [8, Table 3]. Note: N, R, U = normal, rectangular, U-shaped probability distributions.

3.2.2 Model Related Uncertainty

For distances $d < \lambda/2$ the IEC/IEEE 62704-1 [8, section 7.3.3] states that "[...] the only way to determine the uncertainty of the DUT model is by SAR measurements", which is not possible for the given frequency of the DUT. Therefore the procedure was modified by using the squared H-field values instead of SAR/EIAV in [8, equation 14], similar to the assessment for distances $d \geq \lambda/2$ by [8, equation 13].

$$U_{\text{sim,model}} = \max \left(\frac{|H_{\text{ref,n}}^2 - H_{\text{sim,n}}^2|}{H_{\text{ref,max}}^2} \right) \quad (1)$$

$$= \left[\frac{|(1028.96 \text{ A/m})^2 - (1088.04 \text{ A/m})^2|}{(1028.96 \text{ A/m})^2} \right]_{z=6.60 \text{ mm}} \quad (2)$$

$$= 11.81 \% \quad (3)$$

Table 11 shows the budget of the uncertainty contributions of the model parameter. The applicant stated an $k=2$ uncertainty of 1.24 dB \Rightarrow 15.28 % for the measurements done by "cetecom advanced GmbH" (cf. section 1.4), so 7.67 % was used for the $k=1$ uncertainty of the measurement equipment and procedure.

Uncertainty Component	Com-ponent	Section in [8]	Tolerance in %	Probability Distribution	Divisor	c_i	Uncer-tainty in %
Uncertainty of the DUT model		7.3.2 or 7.3.3	11.81 %	N	1	1	11.81 %
Uncertainty of the phantom model		7.3.3	<i>not appl.</i>	N	1	1	<i>not appl.</i>
Uncertainty of the measurement equipment and procedure		-	7.67 %	N	1	1	7.67 %
Combined Std. Uncertainty (k=1)							14.09 %

Table 11: Budget of the uncertainty contributions of the model setup, corresponding to IEC/IEEE 62704-1 [8, Table 4]. Note: N, R, U = normal, rectangular, U-shaped probability distributions.

3.2.3 Model Validation

To validate the numerical model, equation 15 from IEC/IEEE 62704-1 [8, section 7.3.4] was calculated for the H-field line evaluation:

$$E_n = \max \left(\sqrt{\frac{(\nu_{\text{sim,n}} - \nu_{\text{ref,n}})^2}{(\nu_{\text{sim,n}} U_{\text{sim}(k=2)})^2 + (\nu_{\text{ref,n}} U_{\text{ref}(k=2)})^2}} \right) \quad (4)$$

$$= \max \left(\sqrt{\frac{(H_{\text{sim,n}}^2 - H_{\text{ref,n}}^2)^2}{(H_{\text{sim,n}}^2 U_{\text{sim}(k=2)})^2 + (H_{\text{ref,n}}^2 U_{\text{ref}(k=2)})^2}} \right) \quad (5)$$

$$= \left[\sqrt{\frac{((1009.94 \text{ A/m})^2 - (951.95 \text{ A/m})^2)^2}{((1009.94 \text{ A/m})^2 \cdot (23.63 \%))^2 + ((951.95 \text{ A/m})^2 \cdot (15.35 \%))^2}} \right]_{z=7.60 \text{ mm}} \quad (6)$$

$$= 0.41 \leq 1 \quad (7)$$

The condition/inequation is fulfilled, indicating that the deviation is within the expected uncertainty, and hence that the model is valid.

3.2.4 Uncertainty Budget

The budgets for simulation parameters related uncertainties and model related uncertainties were combined ($k=1$) and expanded ($k=2$) for 1g-SAR, 10g-SAR and EIAV as shown in table 12, 13 and 14.

3.2.5 Uncertainty Penalty

The calculated Expanded Std. Uncertainties for SAR/EIAV do not exceed the maximum of 30 % stated in IEC/IEEE 62704-1 [8, Section 7.4]. Therefore uncertainty penalties as described in EN 62311 [10, Section 6.2, Equation 1] were not applied.

3.3 Passive Receiver Impact

In the reported model the phantom is directly placed onto the DUT. However, usually a WPT receiver such as a handset is placed on top of the DUT during charging operation. A receiver would increase the smallest possible approach distance, and its metal parts would act as a shield for the fields, hence decreasing the exposure. To illustrate this effect, an additional simulation was done, whereby a passive phone receiver dummy was added to the model (cf. Figure 11).

Table 15 lists the maximum values for 1g-SAR, 10g-SAR and EIAV for the model with the passive receiver dummy. As expected they are noticeable lower than in case of the reported model. The before mentioned shielding effect also qualitatively changes the SAR/EIAV distribution, as can be seen in Figure 12.

Quantity	Reported Model	With Passive Receiver
$SAR_{1g, max}$	84.2357 mW/kg	0.3126 mW/kg
$SAR_{10g, max}$	40.5715 mW/kg	0.1745 mW/kg
$EIAV_{unaveraged, max}$	15.8004 V/m	0.9106 V/m

Table 15: SAR and EIAV maximum values for the model with the passive receiver dummy.

Uncertainty Component	Section in [8]	Tolerance in %	Probability Distribution	Divisor	c_i	Uncertainty in %
Uncertainty of the DUT model with respect to simulation parameters	7.2	2.41 %	N	1	1	2.41 %
Uncertainty of the developed numerical model of the DUT	7.3	14.09 %	N	1	1	14.09 %
Combined Std. Uncertainty (k=1)						14.29 %
Expanded Std. Uncertainty (k=2)						28.59 %

Table 12: Combined and expanded budget of the 1g-SAR uncertainty, according to IEC/IEEE 62704-1 [8, Table 5]. Note: N, R, U = normal, rectangular, U-shaped probability distributions.

Uncertainty Component	Section in [8]	Tolerance in %	Probability Distribution	Divisor	c_i	Uncertainty in %
Uncertainty of the DUT model with respect to simulation parameters	7.2	2.09 %	N	1	1	2.09 %
Uncertainty of the developed numerical model of the DUT	7.3	14.09 %	N	1	1	14.09 %
Combined Std. Uncertainty (k=1)						14.24 %
Expanded Std. Uncertainty (k=2)						28.48 %

Table 13: Combined and expanded budget of the 10g-SAR uncertainty, according to IEC/IEEE 62704-1 [8, Table 5]. Note: N, R, U = normal, rectangular, U-shaped probability distributions.

Uncertainty Component	Section in [8]	Tolerance in %	Probability Distribution	Divisor	c_i	Uncertainty in %
Uncertainty of the DUT model with respect to simulation parameters	7.2	1.32 %	N	1	1	1.32 %
Uncertainty of the developed numerical model of the DUT	7.3	14.09 %	N	1	1	14.09 %
Combined Std. Uncertainty (k=1)						14.15 %
Expanded Std. Uncertainty (k=2)						28.30 %

Table 14: Combined and expanded budget of the EIAV uncertainty, analogue to the budget of the SAR uncertainty from IEC/IEEE 62704-1 [8, Table 5]. Note: N, R, U = normal, rectangular, U-shaped probability distributions.

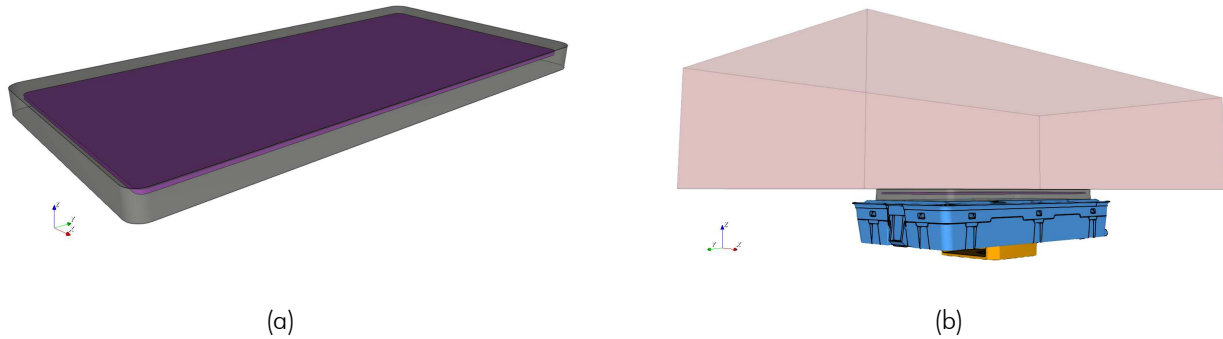


Figure 11: Geometry of the passive receiver dummy, consisting of a 145 · 70 · 7 mm dielectric housing with a metal plate inside (a). The receiver dummy was placed in between DUT and phantom (b).

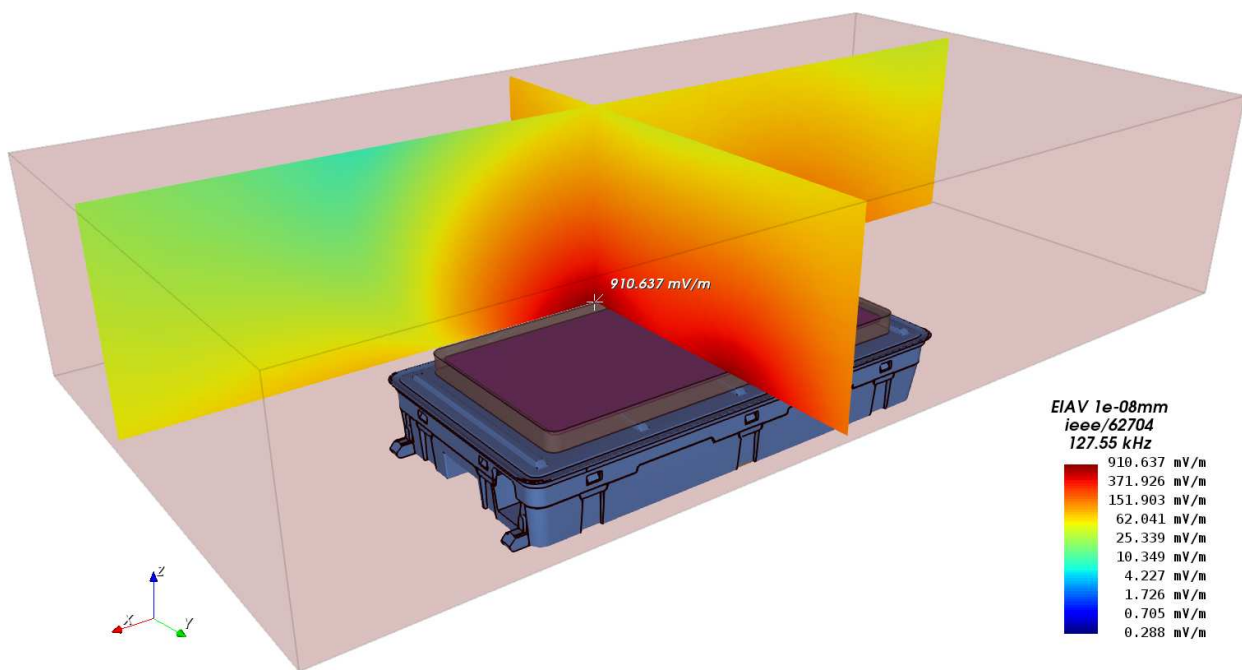


Figure 12: Cutplane through the maximum of the simulated EIAV inside the flat phantom for the model with the passive receiver dummy.

3.4 Conclusion of SAR and EIAV Evaluation

Summarizing the numerical exposure assessment of the DUT, the following can be stated:

1. The investigated scenario (reported model) follows the worst-case assumption that:
 - (a) The flat phantom is in direct contact with the DUT with no WPT receiver present.
 - (b) The DUT is exciting its charging coil with the maximum expectable current, despite the fact that no WPT receiver is present.
 - (c) The search mode duty cycle is neglected.
2. The simulated magnetic field strength and the coil inductance are in good agreement with the measurements (cf. section 2.2), indicating the accurate setup of the numerical model (without phantom).
3. The model validation (cf. section 3.2.3) shows that in-equation 15 from IEC/IEEE 62704-1 is fulfilled, indicating a valid numerical model.
4. The uncertainty analysis returns Expanded Standard Uncertainties below the permissible 30% stated in IEC/IEEE 62704-1 section 7.4.
5. The evaluated exposure quantities are:
 - (a) The evaluated maximum 1g-averaged SAR is 84.2357 mW/kg.
 - (b) The evaluated maximum 10g-averaged SAR is 40.5715 mW/kg.
 - (c) The evaluated maximum EIAV (internal Electric field) is 15.8004 V/m.
6. With respect to the statements above, the conclusion of this numerical exposure assessment report is, that the DUT does not exceed the SAR and/or EIAV exposure limits specified by ICNIRP [1], FCC [2], ISED [3], EUCO [5] and ARPANSA [6]. A tabular evaluation can be found at the beginning of the report.

4 Appendix

4.1 Specific Information for Computational Modelling

Computational resources Computation was performed on 1/4 (split by Numa nodes) of a dual AMD EPYC 7763 64-core processor with 1.253 GB memory usage.

FDTD algorithm implementation and validation cf. [9]

1g-averaged SAR procedures cf. [8, 9]

Total computational uncertainty cf. [9] and section 3.2

Computational parameters for reported model:

Cell Size (min/max): 0.175 mm / 10.37 mm

Domain Size: 550 · 380 · 389 mm

Total amount of mesh cells: approx. 12.7 million

Time step: $2.14245 \cdot 10^{-13}$ s

Total number of time steps: approx. 15 million

Simulation time: approx. 3 hours and 42 minutes

Simulation speed: 13964 million cells per second (13.964 GCells/s)

Excitation method: Gaussian pulse with $f_0 = 0$ Hz, $f_{BW} = 50$ MHz

Phantom model implementation cf. section 3

Tissue dielectric parameters cf. section 3

Transmitter model implementation and validation cf. section 2

Test device positioning cf. section 3

Steady state termination procedures A Gaussian pulse was used for the excitation and the simulation was terminated after the energy had dissipated to more than -101.27 dB.

Test results cf. section 3

4.2 Abbreviations

Abbreviation	Description
CAD	Computer Aided Design
DUT	Device Under Test
EIAV	Averaged Internal Electric Field
EM	Electro Magnetic
FDTD	Finite Difference Time Domain
PCB	Printed Circuit Board
RF	Radio Frequency
RMS	Root Mean Square
SAR	Specific Absorption Rate
S/m	Siemens per meter = $1/(\Omega\text{m})$

Table 16: Abbreviations.

5 References

- [1] International Commission on Non-Ionizing Radiation Protection (ICNIRP), "ICNIRP Guidelines for limiting Exposure to Electromagnetic Fields (100 KHz to 300 GHz)," 2020.
- [2] Federal Communications Commission (FCC, USA), "FCC Radiofrequency radiation exposure limits, 47 C.F.R. § 1.1310," 2020.
- [3] Innovation, Science and Economic Development Canada (ISED, Canada), "RSS-102 Issue 5 - Radio Frequency (RF) Exposure Compliance of Radiocommunication Apparatus (All Frequency Bands)," March 2015.
- [4] ———, "RSS-102 SPR-002 Issue 2 - Supplementary Procedure for Assessing Compliance of Equipment Operating from 3 kHz to 10 MHz with RSS-102," October 2022.
- [5] European Council, "Council Recommendation of 12 July 1999 on the limitation of exposure of the general public to electromagnetic fields (0 Hz to 300 GHz), 1999/519/EC," July 1999.
- [6] Australian Radiation Protection and Nuclear Safety Agency (ARPANSA), "Standard for Limiting Exposure to Radiofrequency Fields – 100 kHz to 300 GHz - Radiation Protection Series S-1, RPS S-1," February 2021.
- [7] IMST GmbH. (2023, March) Empire XPU. Carl-Friedrich-Gauß-Str. 2-4, 47475 Kamp-Lintfort, Germany. [Online]. Available: <http://empire.de>
- [8] "IEC/IEEE International Standard – Determining the peak spatial-average specific absorption rate (SAR) in the human body from wireless communications devices, 30 MHz to 6 GHz - Part 1: General requirements for using the finite-difference time-domain (FDTD) method for SAR calculations," *IEC/IEEE 62704-1:2017*, pp. 1–86, 2017.
- [9] IMST GmbH, "EMPIRE XPU - Code Verification according to IEC/IEEE 62704-1."
- [10] CENELEC, "Assessment of electronic and electrical equipment related to human exposure restrictions for electromagnetic fields (0 Hz to 300 GHz), EN IEC 62311," January 2020.